Feng *et al. Biochar* (2026) 8:55
https://doi.org/10.1007/s42773-026-00572-5

Biochar

ORIGINAL RESEARCH Open Access

Biochar-driven biological regulation dominates acid-hydrolyzable nitrogen accumulation in plantation soils under acid rain stress

Yuanyuan Feng[1,2*†], Yuanhao Liu[1†], Jiaxuan Liu[1], Haibo Hu[1*], Meijia Zhou[1], Yanfang Feng[2] and Lihong Xue[2]

Abstract

Acid-hydrolysable nitrogen (AHN), a crucial fraction of bioavailable soil organic nitrogen (N), is highly sensitive to soil acidification. Alkaline biochar (BC) has been shown to effectively mitigate acid rain (AR)-induced soil acidification. However, its regulatory effects and underlying mechanisms on AHN fractions remain largely unexplored. In this study, a field-scale simulated AR experiment was conducted in a *Quercus acutissima* plantation, utilizing BC derived from *Q. acutissima* litter to evaluate its impacts on AHN fractions and associated soil chemical-biological drivers. The results showed that after 2 years of simulated AR spraying, BC application elevated soil pH by 0.19 units under AR stress and increased total AHN content by 64.8%. Specifically, acid-ammonia N, acid-amino sugar N, acid-amino acid N, and acid-hydrolyzable unidentified N increased by 45.0%, 61.3%, 80.6%, and 60.7%, respectively. BC-amended soils under AR exhibited the highest bacterial network complexity (0.8), whereas fungal network connectivity was reduced. Soil chemo-biological interactions explained 23.1–39.7% of the variations in AHN fractions. Random forest modeling identified microbial N use efficiency as the primary factor influencing acid-ammonia N, and microbial biomass N as the key factor governing the accumulation of acid-amino acid N and acid-amino sugar N. Furthermore, the regulatory effects of BC on AHN fractions (0.77–0.98) surpassed those of AR stress. This study elucidates the mechanistic pathways through which BC modulates acid-induced N dynamics, providing insights for sustainable N management in plantation ecosystems affected by AR.

Highlights

- Biochar increased soil acid-hydrolyzable nitrogen (AHN) by 65% under acid rain (AR).
- Biochar under AR maximized bacterial, but minimized fungal network complexity.
- Soil chemo-biological interactions explained 23-40% of AHN fraction variability.
- Biotic factors outweighed chemical factors in regulating soil AHN fractions.
- Regulatory effects of biochar on soil AHN fractions surpassed those of AR stress.

†Yuanyuan Feng and Yuanhao Liu have contributed equally to this paper.

*Correspondence:
Yuanyuan Feng
Feng.Yuanyuan@hotmail.com
Haibo Hu
hhb@njfu.com.cn
Full list of author information is available at the end of the article

Springer

Keywords Biochar, Acid rain, Plantation soil, Acid-hydrolyzable nitrogen, Bacteria and fungi

Graphical Abstract

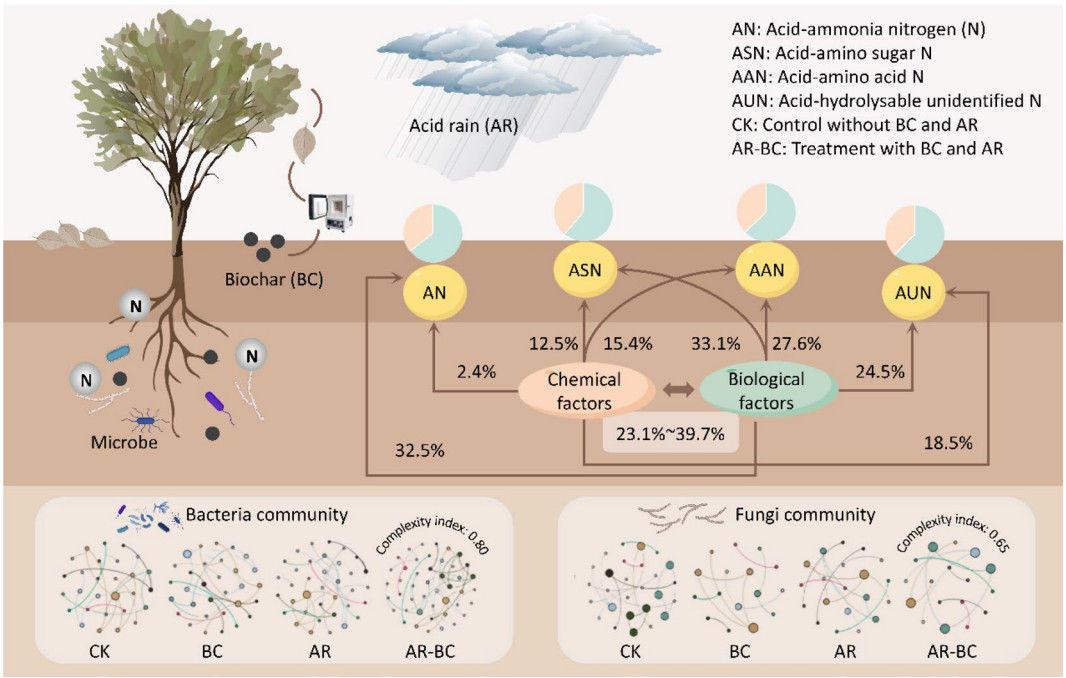

1 Introduction

Nitrogen (N) is an essential nutrient constraining plant and microbial productivity in terrestrial ecosystems (Knorr et al. 2024). It predominantly exists as soil organic N (SON) (accounting for >90% of global soil N), playing central roles in ecosystem functioning and N cycling (Chen et al. 2024a, b). Chemically distinct SON fractions include acid-hydrolyzable N (AHN) and non-hydrolyzable N. AHN serves as the primary bioavailable indicator of soil N supply capacity due to its high sensitivity to environmental perturbations (Lin et al. 2023). Despite the reduced frequency of acid rain (AR) in some regions, the persistence of its legacy effects, including progressive soil acidification, base cation depletion, and aluminum toxicity, continues to threaten the stability and transformation of AHN and the underlying ecosystem functions (Du et al. 2025; Wu et al. 2024; Yu et al. 2025). Therefore, a deeper investigation into the dynamic responses of AHN under AR is crucial for understanding the terrestrial N cycle under global change.

AHN primarily comprises components such as acid-ammonia N (AN), acid-amino acid N (AAN), acid-amino sugar N (ASN), and acid-hydrolyzable unidentified N (AUN) (Xia et al. 2021). Among these, AN can be directly absorbed and utilized by plants and is the primary source of inorganic N. AAN and ASN are derived from soil microbial metabolites and residues. They represent an intermediate pool between stable and available N, exhibiting slow-release characteristics (Ning et al. 2025). AUN, with its complex structure and high stability, plays a crucial role in long-term soil N retention (Lin et al. 2023). AR-induced soil acidification disrupts N mineralization and nitrification, depleting AHN pools (particularly ASN and AAN), exacerbating N leaching, and impairing N fixation (Zhou et al. 2023). These shifts are amplified through altered microbial communities and enzyme activities, which reduce microbial N use efficiency and decouple C-N cycles, ultimately threatening ecosystem productivity (Du et al. 2025; Marinos et al. 2024).

Biochar (BC) emerges as a promising alkaline amendment for AR-affected soils (Arwenyo et al. 2023; Liu et al. 2025). Produced via biomass pyrolysis (300 °C–700 °C), it retains base cations (e.g., Ca^{2+}, Mg^{2+}, and K^{+}) for pH buffering (He et al. 2022; Shi et al. 2019). Meanwhile, BC leverages high surface area and cation exchange capacity to enhance NH_4^+ adsorption, thereby prolonging soil N retention (Toczydlowski et al. 2023). Furthermore, BC modulates C-N enzyme (e.g., β-glucosidase (BG) and

leucine aminopeptidase (LAP)) activities and associated microorganisms (e.g., N cycle-related bacteria and fungi) to regulate N transformation pathways (Liu et al. 2021; Yang et al. 2025). Given the differences in bioavailability among AHN components, their responses to AR stress and BC application may exhibit heterogeneity. However, the regulatory effects of BC on AHN fractions under AR conditions and their underlying mechanisms remain largely unexplored. We hypothesized that BC may preferentially stimulate active AHN fractions (i.e., AN, ASN, and AAN) by reconfiguring chemo-biological interactions under AR stress.

Herein, an in situ AR simulation platform in *Quercus acutissima* plantations was established, with *Q. acutissima* litter-derived BC applied to assess its effects on soil AHN fractions, enzyme activities, microbial biomass, and microbial communities. The objectives of this study were to: (1) reveal the effects of BC and AR stress interaction on soil AHN fractions; (2) analyze the dominant chemical and biological factors, as well as the mechanisms governing BC-mediated AHN regulation under AR stress. Our findings will provide a scientific basis for developing targeted strategies using BC for soil N management and ecological restoration in AR-affected ecosystems.

2 Materials and methods

2.1 Preparation of BC and simulated AR solution

The BC was produced from *Q. acutissima* leaf litter collected at Xiashu forest farm (Nanjing, China). The feedstock underwent oxygen-limited pyrolysis at 500 °C for 2 h in a muffle furnace. The resulting BC was then cooled, homogenized by sieving through a 2-mm mesh, and stored for use. The concentrations of metallic elements (K, Ca, Mg, Fe, Mn, Cu, and Zn) were determined using inductively coupled plasma optical emission spectrometry (ICP-OES, PerkinElmer Optima 8000, USA) following acid digestion. The specific surface area (SSA), pore size, and pore volume were determined from N adsorption–desorption isotherms using the Brunauer–Emmett–Teller method (Micromeritics ASAP 2460, USA) (Wang et al. 2025). The BC properties were characterized as follows: pH, 10.0; Organic carbon (OC), 589.8 g kg^{-1}; Total N (TN), 4.6 g kg^{-1}; K, 5.7 g kg^{-1}; Ca, 8.4 g kg^{-1}; Mg, 5.4 mg kg^{-1}; Fe, 230.1 mg kg^{-1}; Mn, 193.0 mg kg^{-1}; Cu, 64.7 mg kg^{-1}; Zn, 51.1 mg kg^{-1}; specific surface area (SSA), 1.8 m^2 g^{-1}; average pore size, 1.375 nm; and average pore volume, 0.008 cm^3 g^{-1}.

Based on AR composition evolution in the North Subtropical Region of China, where the sulfate-nitrate mixed type is shifting to the nitrate-dominant type, nitrate-based AR was simulated (Zhou et al. 2023). The stock solution was prepared by mixing 0.5 mol L^{-1} H_2SO_4 and 0.5 mol L^{-1} HNO_3 at a SO_4^{2-}:NO_3^- molar ratio of 1:5, followed by dilution with deionized water to a final pH of 4.5. The concentration of NO_3^--N concentration in the applied AR solution was 0.316 g N L^{-1}.

2.2 Experimental design

The experiment was conducted at the Yangtze River Delta Farmland Shelterbelt Ecosystem Observatory (32°7′49′′N, 119°12′7′′E), Jiangsu Province, China. This region experiences a subtropical monsoon climate with a mean annual temperature of 15.1 °C and precipitation of 1184.3 mm. The site (elevation: 180 m) features hilly terrain with yellow-brown soils characterized by the following properties: bulk density, 1.4 g cm^{-3}; moisture content, 14.6%; soil pH, 5.0; organic matter (OM), 11.1 g kg^{-1}; SOC, 33.5 g kg^{-1}; and TN, 3.2 g kg^{-1}.

A *Q. acutissima* plantation with a mean height of 15 m and density of 430 trees ha^{-1} was selected for the study. Twelve plots (3 m × 3 m) were established in a completely randomized block design, with the spatial distribution of the plots shown in Fig. S1. To prevent lateral leaching and cross-treatment interference, each plot was isolated by PVC barriers (30 cm in height and 0.5 cm in thickness), installed to a depth of 25 cm (leaving 5 cm above ground). A 3-m buffer zone was maintained between adjacent plots. The experiment consisted of four treatments, each with three replicates: (1) Control (CK): no BC, sprayed with deionized water; (2) BC application only (BC): BC applied, sprayed with deionized water; (3) AR spraying only (AR): no BC, sprayed with simulated AR; and (4) BC and AR (AR-BC): BC applied, sprayed with simulated AR.

In June 2021, BC was surface-applied at a rate of 0.5 kg m^{-2} to BC and AR-BC plots and lightly incorporated into the topsoil. To isolate the impacts of AR from the effect of water input, all plots received spray applications of equal volumes of liquid. The CK and BC treatments were sprayed with deionized water, while the AR and AR-BC treatments were sprayed with simulated AR. From June 2021 to June 2022, the simulated AR was applied monthly. The application volume per event was designed to reflect local monthly precipitation patterns, corresponding to a water depth of 11.1 mm in June, 11.8 mm in July, and 9.2 mm in August, with amounts in other months ranging from 2.0 mm to 5.2 mm. The details shown in Fig. S2.

2.3 Soil AHN fractions

Surface soil samples (0–10 cm depth) were collected in June 2022 using a five-point sampling method. After removing stones, roots, litter, and visible BC particles, samples were processed for subsequent measurements. Soil AHN fractions were quantified via a modified acid hydrolysis method described by Ren et al. (2023). Briefly,

soil samples were digested with 6 mol L^{-1} HCl for 12 h. Total AHN content was quantified by Kjeldahl steam distillation after H_2SO_4 digestion. Soil AN content was measured by MgO oxidation distillation. AAN content was quantified via ninhydrin oxidation coupled with phosphate-borate buffer steam distillation. ASN content was assessed through steam distillation under phosphate-borate buffer (pH = 11.2). AUN content was calculated as the difference between AHN and the sum of AN, AAN, and ASN. NHN content was determined as the difference between soil TN and AHN.

2.4 Soil basic chemical properties

Soil pH and electrical conductivity (EC) were measured using a pH meter (Sartorius GmbH, Göttingen, Germany) and a conductivity meter (Universal Conductivity Meter, Ghm Group, Germany), respectively. SOC and TN contents were determined with an elemental analyzer (Vario EL III, Elementar, Germany). Dissolved organic C (DOC) and dissolved total N (DTN) were quantified via 0.5 M K_2SO_4 extraction followed by analysis on a TOC analyzer (TOC-VCPH, Shimadzu, Japan). Soil exchangeable calcium was determined by extraction with 1 mol L^{-1} ammonium acetate, and the concentration in the extract was quantified by inductively coupled plasma optical emission spectrometry (ICP-OES, PerkinElmer Optima 8000, USA).

2.5 Soil enzyme activity, microbial metabolic efficiency and microbial biomass

Activities of soil BG, β-N-acetylglucosaminidase (NAG), and acid phosphatase (AP) were quantified using nitrophenol-based colorimetric assays. Soil LAP activity was determined via fluorogenic substrate methods (Xia et al. 2025).

Soil microbial C use efficiency (CUE) and N use efficiency (NUE) were calculated based on ecological stoichiometry using the following equations (Sinsabaugh et al. 2016; Sun et al. 2022):

$$CUE = CUE_{max} \times \frac{S_{C:N}}{(K + S_{C:N})}$$

$$S_{C:N} = \frac{1}{EEA_{C:N}} \times \frac{B_{C:N}}{L_{C:N}}$$

$$NUE = NUE_{max} \times \frac{S_{N:C}}{(K + S_{N:C})}$$

$$S_{N:C} = (1 - EEA_{N:C}) \times \frac{B_{N:C}}{L_{N:C}}$$

CUE_{max} and NUE_{max} represent the theoretical maximum C and N supply rates for microbial growth, set at 0.6 and 1.0, respectively. The saturation constant K was assigned a value of 0.5. $EEA_{C:N}$ and $EEA_{N:C}$ represent the C: N and N: C ratios of total extracellular enzyme activity, respectively. $B_{C:N}$ and $B_{N:C}$ refer to the C: N and N: C ratios of microbial biomass, respectively. $L_{C:N}$ and $L_{N:C}$ represent the C: N and N: C ratios of soil OM, respectively.

To further explore the transition between C and N limitation in soil microbial metabolism reflecting the relative efficiency of C versus N utilization under specific resource conditions, the Threshold Element Ratio (TER) was calculated using the equation of Mooshammer et al. (2014):

$$TER = \frac{NUE}{CUE} \times B_{N:C}$$

$B_{N:C}$ represents the N to C ratio of ecological enzyme activity.

Soil microbial biomass C (MBC) and microbial biomass N (MBN) were determined using the chloroform fumigation extraction method (Li et al. 2023).

2.6 Soil microbial sequencing and functional prediction

Soil DNA was extracted using the FastDNA™ Spin Kit (MP Biomedicals, USA), with concentration and purity assessed via NanoDrop 2000. The bacterial 16S rRNA V3-V4 region was amplified with primers *341F* and *806R*, while the fungal ITS region was amplified with *ITS1F* and *ITS2R*. PCR products were verified by agarose gel electrophoresis, purified, and sequenced on the Illumina MiSeq PE250 platform. Bioinformatic processing employed the QIIME2 pipeline. Based on the SILVA database (bacteria) and the UNITE database (fungi), operational taxonomic units (OTUs) with 97% similarity were clustered and taxonomically annotated. Soil bacterial functional potential was predicted via Phylogenetic Investigation of Communities by Reconstruction of Unobserved States (PICRUSt2) with Kyoto Encyclopedia of Genes and Genomes (KEGG) pathway mapping. Soil fungal function was predicted using FUNGuild for ecological trait annotation.

2.7 Statistical analysis

Statistical analysis was performed using SPSS 20.0 software (SPSS Inc., Chicago, IL, USA). Differences between treatment groups were assessed using one-way analysis of variance (ANOVA), followed by post hoc comparisons with Duncan's multiple range test (mean ± SD). The Mantel Test was performed using the "ade4" R package to assess correlations between soil chemical and biological factors with soil AHN fractions. Variance decomposition analysis (VPA) based on Hellinger transformation statistics was employed to determine the independent and combined contributions of soil chemical and biological variables in explaining the variation in AHN fractions. The random forest (RF) model was constructed using the

"randomForest" R package to identify essential predictors influencing AHN fractions. The partial least squares path model (PLS-PM) was developed using the "plspm" R package to elucidate the direct and indirect effects of BC application, AR stress, and soil factors on AHN fractions.

3 Results

3.1 Effects of BC on soil ANH fractions under AR stress

Figure 1a shows that the TN content of AR was significantly reduced by 37.2% compared to CK ($p < 0.05$), while the TN content of AR-BC was 2.03 times that of BC. The AR-BC treatment significantly increased soil AHN content by 55.6% compared to BC and by 64.8% relative to AR, and the AHN content of AR was reduced by 33.7% compared to CK ($p < 0.05$, Fig. 1b). Soil AN and ASN contents of AR-BC were 45.0% and 61.3% higher than those of AR, respectively ($p < 0.05$, Fig. 1c, d). Concurrently, AR-BC markedly enhanced AAN content, with increases of 67.5% over BC and 80.6% over AR ($p < 0.05$, Fig. 1e). Compared to BC and AR treatments, AR-BC significantly raised AUN levels by 30.0% and 60.7%, respectively ($p < 0.05$, Fig. 1f).

3.2 Effects of BC on soil basic chemical properties under AR stress

Compared to CK and AR, the AR-BC treatment significantly increased soil pH by 0.05 units and 0.19 units, respectively ($p < 0.05$, Fig. 2a). Both AR and AR-BC treatments increased soil EC by 42.0% and 27.4% compared to CK ($p < 0.05$, Fig. 2b). Relative to AR, AR-BC increased SOC content by 62.7% ($p < 0.05$, Fig. 2c). The AR-BC treatment significantly reduced DOC by 28.8% and 14.0% compared to BC and AR, respectively ($p < 0.05$, Fig. 2d). The BC treatment decreased DTN by 11.5% compared to CK, while AR-BC reduced DTN by 11.4% relative to AR ($p < 0.05$, Fig. 2e).

3.3 Effects of BC on soil enzyme activity, microbial metabolic efficiency and microbial biomass under AR stress

Compared to CK, the AR-BC treatment significantly reduced soil BG activity by 19.9% ($p < 0.05$, Fig. 2f). Compared to CK and AR, AR-BC treatment significantly reduced soil NAG activity by 35.7% and 54.4%, respectively ($p < 0.05$, Fig. 2g). Soil LAP activity was significantly increased by 47.9% and 15.6% in AR-BC compared to CK and AR ($p < 0.05$, Fig. 2h). The AR-BC treatment significantly decreased soil AP activity by 53.2% and 35.7% compared to CK and AR, respectively ($p < 0.05$, Fig. 2i). The AR-BC treatment significantly increased soil CUE by 41.8% relative to AR ($p < 0.05$, Fig. 2j). Meanwhile, the AR-BC treatment increased soil NUE by 21.4% compared to AR ($p < 0.05$, Fig. 2k). AR exhibited significantly higher TER than the BC and AR-BC treatments ($p < 0.05$, Fig. 2l).

Regarding microbial biomass, the AR-BC treatment significantly increased soil MBC by 92.3% compared to AR ($p < 0.05$, Fig. 3a). AR-BC significantly increased soil MBN content by 62.9% in comparison with AR ($p < 0.05$, Fig. 3b). Linear regression analysis revealed a positive correlation between AN and MBN ($R^2 = 0.46$, $p < 0.05$, Fig. 3c). Soil MBN exhibited positive correlations with ASN ($R^2 = 0.36$, $p < 0.05$, Fig. 3d) and AAN ($R^2 = 0.68$, $p < 0.001$, Fig. 3e). There was no significant correlation between soil MBN and AUN ($R^2 = 0.25$, $p > 0.05$, Fig. 3f). Soil SOC showed a significant positive correlation with MBC ($R^2 = 0.54$, $p < 0.01$, Fig. 3g). A significant positive correlation was observed between MBN and TN ($R^2 = 0.64$, $p < 0.01$, Fig. 3h).

3.4 Effects of BC on the structure and function of soil bacterial and fungal communities under AR stress

Figure 4a shows that Acidobacteriota and Proteobacteria were the dominant bacterial phyla, collectively accounting for 68.6–83.3% of total sequences. AR significantly altered the relative abundances of Acidobacteriota, Proteobacteria, Actinobacteriota, and Chloroflexi ($p < 0.05$, Fig. S4). Under AR conditions, BC application reduced the abundance of Acidobacteriota by 17.2% while increasing the abundance of Proteobacteria by 12.9% ($p < 0.05$). Soil fungal communities were primarily composed of Basidiomycota, Unnamed taxa, Ascomycota, and Unassigned lineages (Fig. 4b). Both BC ($p < 0.05$) and AR ($p < 0.001$) significantly influenced the abundance of Basidiomycota (Fig. S5). Figure 4c shows that bacterial co-occurrence networks exhibited the highest complexity under AR with BC (complexity index: 0.8; 45 nodes, 36 edges). In contrast, fungal networks showed reduced complexity (complexity index: 0.65) under the same treatment (Fig. 4d).

Bacterial metabolic pathways remained unaltered under BC application without AR stress ($p > 0.05$, Fig. 4e). Critically, under AR stress, BC significantly suppressed five pathways while enhancing two others ($p < 0.05$, Fig. 4f). Specifically, compared to CK, AR-BC upregulated Anchor biosynthesis and Spliceosome pathways but downregulated mRNA surveillance pathway, Basal transcription factors, Cell cycle, Hepatitis C, and Pancreatic cancer pathways (Fig. 4g). Fungal functional predictions revealed that BC significantly affected three ecological guilds, including Epiphyte-Plant Pathogen, Ectomycorrhizal-Fungal Parasite-Soil Saprotroph-Undefined Saprotroph and Wood Saprotroph ($p < 0.05$, Fig. 4h, i). The effects of these functions under AR stress and non-AR conditions exhibited opposing patterns (Fig. 4j).

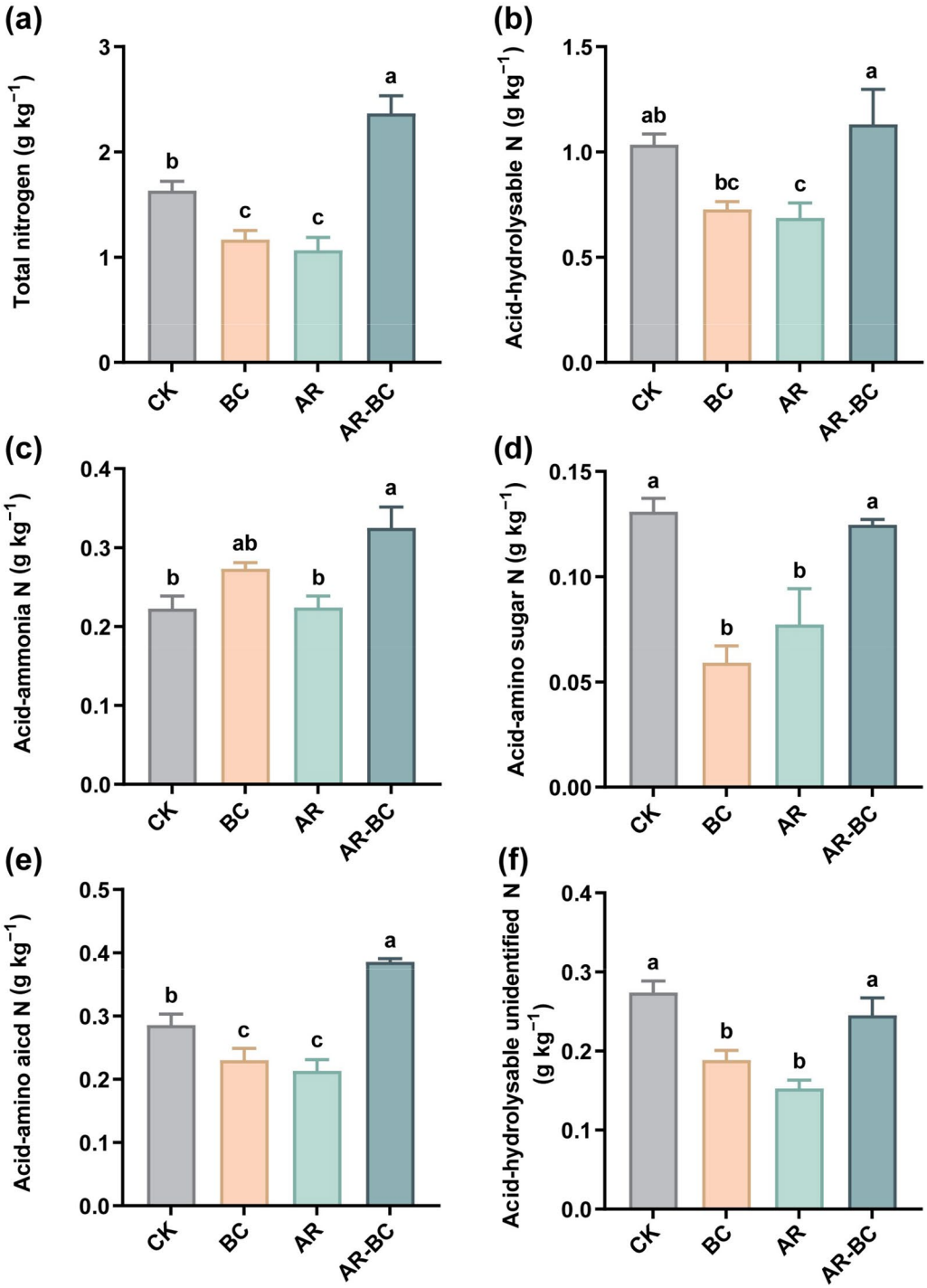

Fig. 1 Soil nitrogen (N) pool contents among all treatments. **a** Total N; **b** Acid-hydrolysable N; **c** Acid-ammonia N; **d** Acid-amino sugar N; **e** Acid-amino acid N; **f** Acid-hydrolysable unidentified N. BC, biochar; AR, Acid rain; AR-BC, Treatment with BC and AR; CK, Control without BC and AR. Different lowercase letters represent significant differences, according to Duncan's test ($p < 0.05$)

3.5 Soil chemo-biological factors of AHN fractions

As shown in Fig. 5a, soil AN content was positively correlated with SOC (r = 0.58, $p < 0.01$), TN (r = 0.48, $p < 0.01$), DTN (r = 0.48, $p < 0.01$), MBC (r = 0.43, $p < 0.01$), MBN (r = 0.41, $p < 0.01$), LAP (r = 0.39, $p < 0.01$), and AP (r = 0.32, $p < 0.05$). Soil ASN and AAN content were

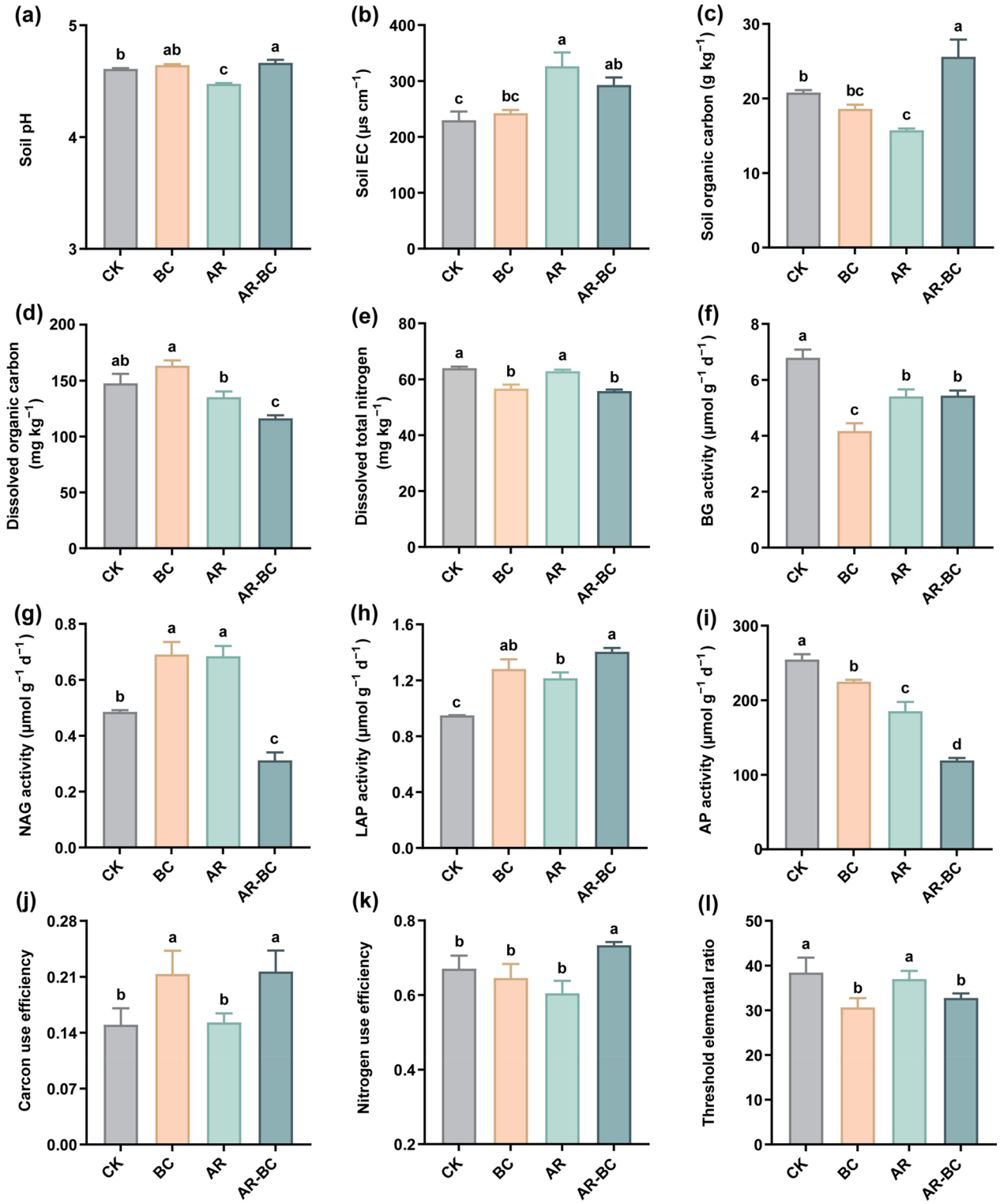

Fig. 2 Soil basic chemical properties, enzyme activity and carbon (C) and nitrogen (N) use efficiency among all treatments. **a** Soil pH; **b** Soil electrical conductivity (EC); **c** Soil organic C; **d** Dissolved organic C; **e** Dissolved total N; **f** β−1,4-glucosidase (BG) activity; **g** β-N-acetyl glucosaminidase (NAG) activity; **h** Leucine aminopeptidase (LAP) activity; **i** Acid phosphatase (AP) activity; **j** C use efficiency; **k** N use efficiency; **l** Threshold elemental ratio. BC, biochar; AR, Acid rain; AR-BC, Treatment with BC and AR; CK, Control without BC and AR. Different lowercase letters represent significant differences, according to Duncan's test ($p < 0.05$)

primarily influenced by MBN (r = 0.47 and 0.60, $p < 0.01$) and NAG (r = 0.54 and 0.81, $p < 0.01$). Additionally, soil AUN content was significantly correlated with pH (r = 0.39, $p < 0.05$), SOC (r = 0.28, $p < 0.05$), TN (r = 0.28, $p < 0.05$), NAG (r = 0.34, $p < 0.05$), and NUE (r = 0.26, $p < 0.05$).

Soil TN content showed significant positive correlations with SOC (r = 0.93, $p < 0.001$), MBC (r = 0.88, $p < 0.001$), MBN (r = 0.87, $p < 0.001$), and NUE (r = 0.70, $p < 0.05$). Meanwhile, TN was significantly negatively correlated with DOC (r = −0.59, $p < 0.05$), NAG (r = −0.93, $p < 0.001$), and AP (r = −0.59, $p < 0.05$). Soil MBN was influenced by SOC (r = 0.83, $p < 0.001$), DOC (r = −0.58, $p < 0.05$), MBC (r = 0.91, $p < 0.001$), NAG (r = −0.87, $p < 0.001$), AP (r = −0.70, $p < 0.05$), and NUE (r = 0.86, $p < 0.001$). NUE was significantly correlated with pH (r = 0.62, $p < 0.05$), SOC (r = 0.76, $p < 0.01$), MBC (r = 0.79, $p < 0.01$), and NAG (r = −0.69, $p < 0.05$).

Figure 5b shows that the contribution rates of soil chemical and biological factors to soil AN were 2.4% and 32.5%, respectively. The combined contribution rate of soil chemical and biological factors to soil ASN was 36.7% (Fig. 5c). The chemo-biological interaction explained 39.7% of the variation in soil AAN (Fig. 5d). The explanation rates of soil chemical and biological factors to soil AAN were 15.4% and 27.6%, respectively. The explanation rate of biological factors (24.5%) on soil AUN exceeded that of chemical factors (18.5%), with their interaction explaining 37.7% (Fig. 5e).

3.6 Dominant drivers influencing soil ANH fractions

Figure 6a shows that soil DTN was the dominant predictor of BC-induced changes in soil AN, with a relative importance of 7.2%. Soil chemical and biological factors explained 34.2% and 65.8% of AN variations, respectively. Soil MBN showed the highest predictive power for ASN (7.2%), followed by LAP (6.4%) and TN (6.0%) (Fig. 6b). Concurrently, LAP, DTN, and MBN were identified as the primary predictors of AAN, with contribution rates of 7.6%, 6.7% and 6.5%, respectively (Fig. 6c). Soil NAG activity exhibited the strongest influence (5.7%) in soil AUN modulation (Fig. 6d).

3.7 Pathway analysis of BC effects on soil ANH fractions under AR stress

PLS-PM models demonstrated excellent fit, with goodness-of-fit indices ranging from 0.55 to 0.77, explaining 70%, 89%, 91%, and 90% of the variance in AN, ASN, AAN, and AUN, respectively (Fig. 7). Figure 7a shows that BC directly affected soil AN content ($\lambda = 0.86$, $p < 0.05$). Meanwhile, BC indirectly promoted soil AN by increasing soil pH ($\lambda = 0.73$, $p < 0.05$) and NUE ($\lambda = 0.58$, $p < 0.05$). BC increased soil LAP activity ($\lambda = 0.77$, $p < 0.05$) and MBN content ($\lambda = 0.65$, $p < 0.05$), thereby promoting soil ASN accumulation ($\lambda = 0.76$ and 0.86, $p < 0.01$, Fig. 7b). BC increased soil MBN content ($\lambda = 0.64$, $p < 0.05$), thereby indirectly leading to the accumulation of soil AAN content ($\lambda = 0.81$, $p < 0.01$, Fig. 7c). BC application exhibited a significant negative correlation with soil AUN content ($\lambda = -0.43$, $p < 0.05$, Fig. 7d). The total effects of BC application on soil AN, ASN, AAN, and AUN were 0.98, 0.77, 0.92, and 0.80, respectively. They were higher than corresponding values under AR stress (0.57, 0.09, 0.09, and 0.31, Fig. 7e).

4 Discussion

4.1 BC-mediated accumulation of soil AHN under AR stress

This study demonstrates the promotive effect of BC on soil AHN under AR stress. While AR significantly reduced soil TN content (Fig. 1), likely due to enhanced mineral N leaching and suppressed SON accumulation (Du et al. 2025), BC application effectively mitigated this TN loss. The decline in TN under AR stress typically corresponds to a depletion of the SON pool and a parallel decrease in AHN fractions, including AN, AAN, ASN, and AUN (Ning et al. 2025). In contrast, the recovery of TN induced by BC coincided with the restoration and augmentation of these AHN components (Fig. 8). These findings underscore the critical role of BC in enhancing soil N availability and maintaining the stability of the N cycle, highlighting its potential utility in mitigating environmental stressors such as AR.

The absence of a significant difference in AN content between the AR and CK treatments indicates that the direct input of NO_3^- from AR was not the primary factor for AN accumulation (Fig. 1). Consequently, the pronounced increase in AN observed in the AR-BC treatment originates from shifts in internal soil N

(See figure on next page.)

Fig. 3 Soil microbial biomass among all treatments. **a** Microbial biomass carbon (MBC). **b** Microbial biomass nitrogen (MBN). Different lowercase letters represent significant differences, according to Duncan's test ($p < 0.05$). Relationships between MBN and **c** acid-ammonia N, **d** acid-amino sugar N, **e** acid-amino acid N, and **f** acid-hydrolysable unidentified N. **g** Relationships between MBC with soil organic C and dissolved organic C. **h** Relationships between MBN with soil total N and dissolved total N. The solid lines represent the significant linear fit at $p < 0.05$ and the dashed lines represent the insignificant linear fit at $p > 0.05$

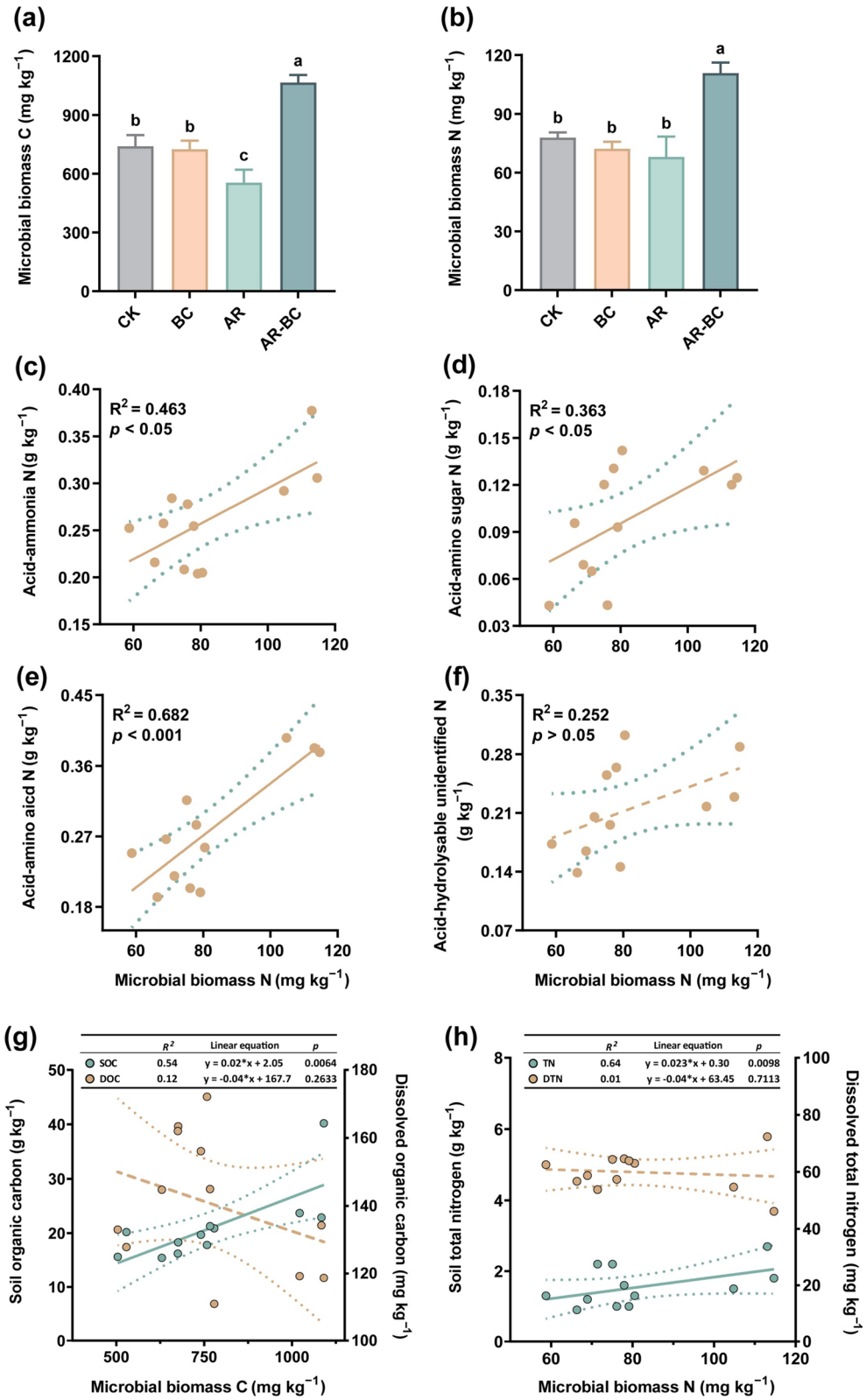

Fig. 3 (See legend on previous page.)

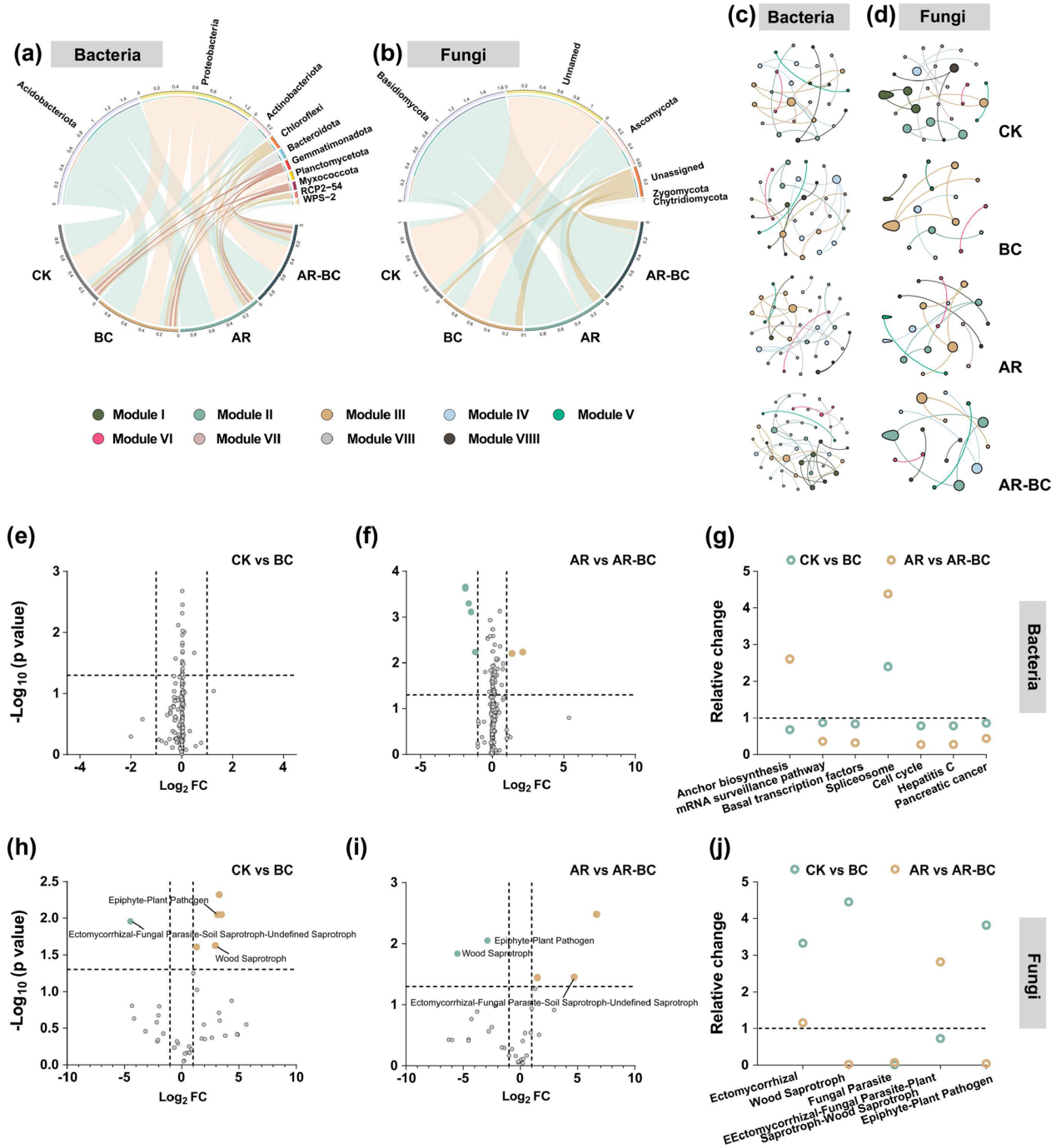

Fig. 4 Soil microbial community structure and predicted function among all treatments. **a** Top 10 soil bacterial phyla in relative abundance. **b** Top 6 soil fungi phyla in relative abundance. **c** Co-expression network diagram of soil bacteria community. **d** Co-expression network diagram of soil fungi community. Variation of soil bacteria community predicted function between CK and BC **e**, as well as AR with AR-BC **f**. Variation of soil fungi community predicted function between CK and BC **h**, as well as AR with AR-BC **i**. Relative changes of soil bacteria (**g**) and fungi (**j**) community predicted function between CK and BC, as well as AR with AR-BC. Predicted functions with 2 times significant changes are highlighted in the volcano plots

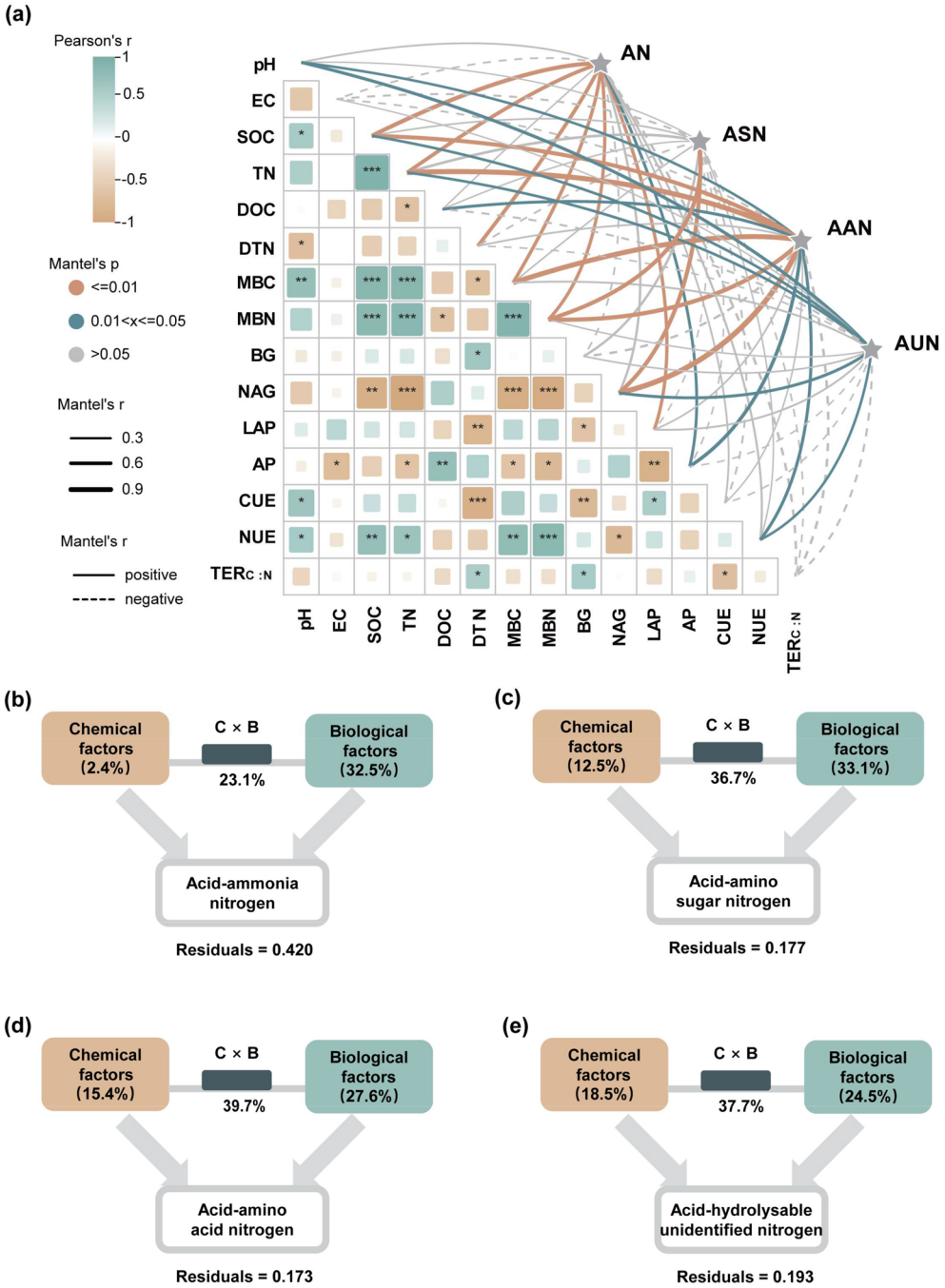

Fig. 5 **a** Relationships between soil chemical with biological factors, and their effects on soil acid-hydrolysable nitrogen (N). Asterisks (*, ** and ***) indicate significant differences ($p < 0.05$, < 0.01, and < 0.001). Individual and joint variance contributions of soil chemical and biological properties to soil acid-ammonia N **b**, acid-amino sugar N **c**, acid-amino acid N **d,** and acid-hydrolysable unidentified N **e**. Percentages indicate the individual and interaction joint explanatory rates of each indicator on soil acid-hydrolysable N fractions

transformation processes, likely induced by the interaction between BC and AR. This interaction may presumably alter the soil microenvironment, impacting microbial community structure and the activity of enzymes governing N mineralization and nitrification (Tables S1-S4). We propose that the increased AN primarily resulted from enhanced microbial turnover and the release of N from acid-labile organic compounds under AR stress.

The significantly higher AHN accumulation under the AR-BC treatment, compared to BC or AR alone (Fig. 1),

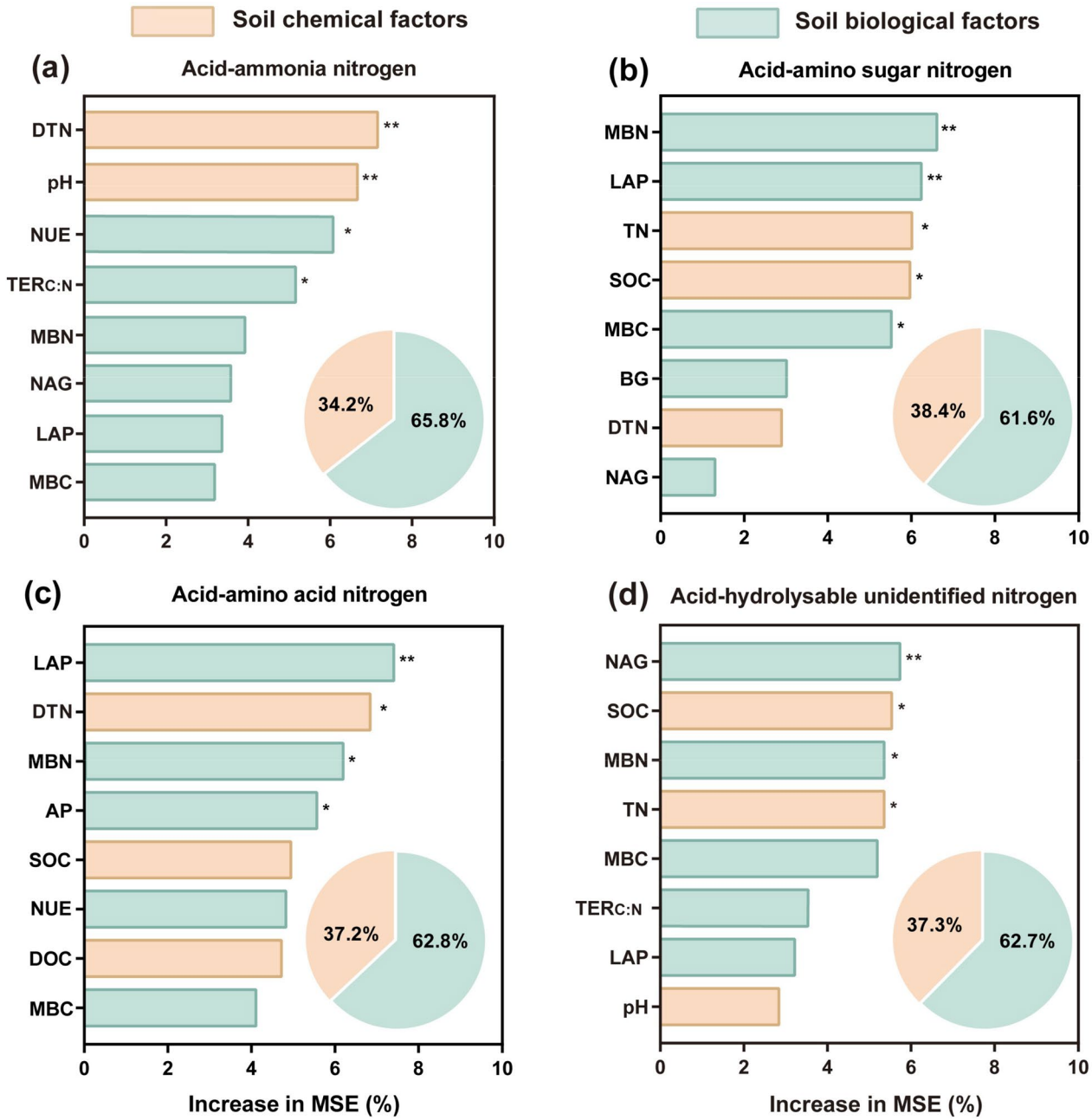

Fig. 6 Important factors affecting soil acid-ammonia nitrogen (N) **a**, acid-amino sugar N **b**, acid-amino acid N **c**, and acid-hydrolysable unidentified N **d**. Asterisks (* and **) indicate significant differences ($p < 0.05$ and < 0.01). Percentages in the pie charts indicate the percentage of soil chemical and biological factors contributing to soil acid-hydrolysable N fractions. EC, electrical conductivity; SOC, soil organic C; TN, total N; DOC, dissolved organic C; DTN, dissolved total N; MBC, microbial biomass C; MBN, microbial biomass N; BG, β-1,4-glucosidase; NAG, β-N-acetyl glucosaminidase; LAP, leucine aminopeptidase; AP, acid phosphatase; CUE, C use efficiency; NUE, N use efficiency; TER, threshold elemental ratio

likely results from a synergistic interaction between N supply and retention mechanisms. AR provides a continuous input of nitrate, which enlarges the soil N substrate pool, while BC elevates soil pH and buffering capacity, alleviating acid stress and improving microbial habitat (Feng et al. 2025). This may enhance microbial N use efficiency and promote the transformation and stabilization of N, leading to greater retention within the AHN fraction (Lee et al. 2025). In contrast, AR alone promotes leaching and acidification, limiting net AHN accumulation, whereas BC alone is constrained by limited native N availability.

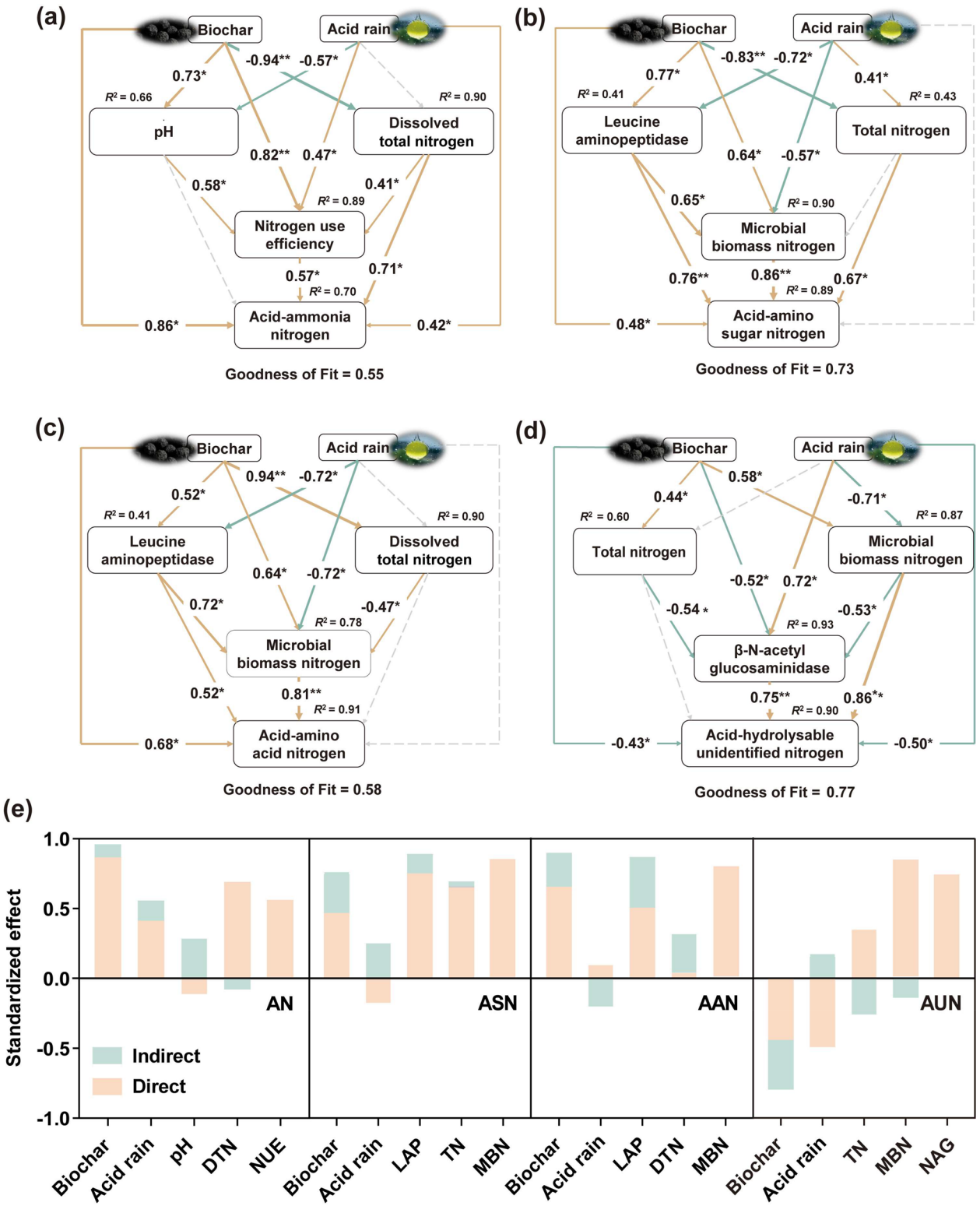

Fig. 7 Effects of different chemical and biological factors on soil acid-ammonia nitrogen (N) **a**, acid-amino sugar N **b**, acid-amino acid N **c**, and acid-hydrolysable unidentified N **d**, based on partial least squares path modeling. **e** Standard effects of soil chemical and biological properties on soil acid-hydrolysable N fractions. Orange and green colors indicate significant positive and negative effects ($p < 0.05$) between the two variables, respectively. The dashed lines indicate no significant effect ($p > 0.05$). Asterisks (* and **) indicate significant differences ($p < 0.05$ and $p < 0.01$)

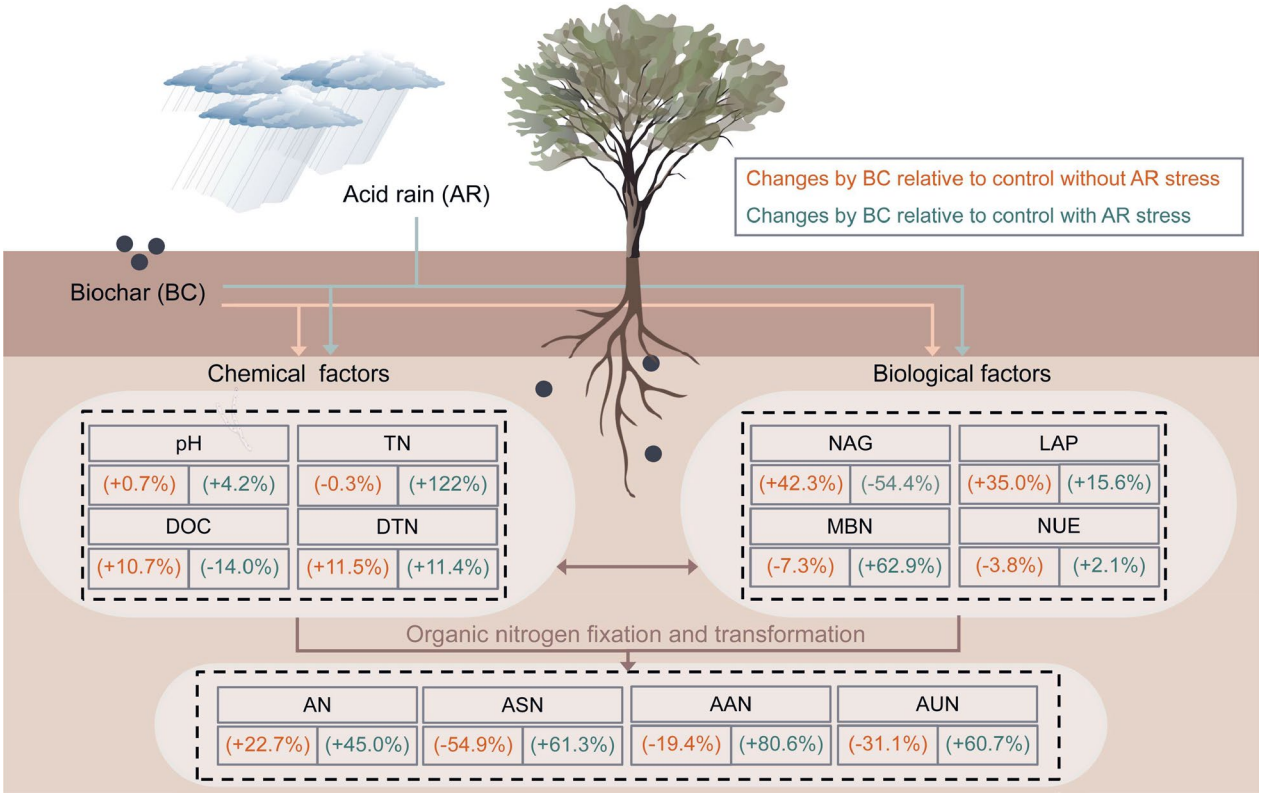

Fig. 8 Conceptual diagram of biochar (BC) amendment effects on soil acid-hydrolyzed nitrogen (N) fractions under acid rain (AR) and non-acid rain stress conditions. Orange and green numbers indicate ercentage changes relative to soil control without and with AR stress, respectively

The differential stimulation of AN and ASN by BC contrasts with the findings of Wang et al. (2023), likely attributable to feedstock-specific properties (Qi et al. 2024). On one hand, *Q. acutissima* leaf-derived BC exhibits high ash content and SSA, enhancing its capacity to adsorb free AN and ASN in soil, thereby promoting their accumulation (Liu et al. 2025; Shi et al. 2019). On the other hand, the macropore-rich structure of BC may improve soil aeration and microbial activity, fostering microbial residue accumulation and ASN production (Jia et al. 2024).

Under AR stress, BC application significantly increased soil AAN content (Fig. 1), a result diverging from Zhang et al. (2022). This discrepancy may stem from differences in BC application rates. Low-dose BC can effectively improve soil nutrient status and OM content, providing microorganisms with abundant nutrient resources to enhance metabolic residue accumulation (Cheng et al. 2023). Nevertheless, high-dose BC may disrupt soil nutrient ratios, inhibiting microbial assimilation of OM and reducing microbial-derived N production (Chen et al. 2024a, b). These findings highlight a dose-dependent relationship between BC application and N transformation processes. Future studies should quantify dose-dependent mechanisms of BC in regulating N cycling within AR-stressed plantation soils, enabling field-relevant optimization across environmental gradients.

4.2 Soil chemo-biological drivers influencing soil AHN accumulation under AR stress

The BC application significantly increased soil LAP activity under AR stress (Fig. 2). We propose that concurrent reduction in soil DTN may compel microbes toward enzymatic N acquisition (Li et al. 2024). This is evidenced by the significant negative correlation between soil LAP activity and DTN content (Fig. 5). This metabolic compensation might enhance NUE through BC-mediated microbial optimization (Xu et al. 2025). BC application significantly increased soil MBC and MBN contents under AR stress (Fig. 3), which contrasts with the findings of Jia et al. (2024). This may be attributed to carbonate buffering and niche specialization (Liu et al. 2025; Yang et al. 2025). Firstly, BC ash may neutralize acidity via $CO_3^{2-} + 2H^+ \rightarrow 2H_2O + CO_2$, alleviating acid inhibition on microbiota (Arwenyo et al. 2023; Liu et al. 2025). Secondly, BC may promote diazotrophs and ammonia-oxidizing bacteria (e.g., *AOB*) (Shi et al. 2019), boosting

microbial N assimilation (Chen et al. 2024a, b; He et al. 2022).

Under AR stress, BC amendment promoted a marked restructuring of the microbial community toward bacterial dominance. This transition was evidenced by a distinct peak in bacterial network complexity in the AR-BC treatment, which contrasted sharply with the concurrent simplification of the fungal network topology (Fig. 4). Such topological divergence highlights a specialized ecological response of the fungal community to multiple stressors. On one hand, such network simplification may reflect weakened interspecific interactions and a concentration of associations among a few core taxa, leading to increased functional specialization (Silverstein et al. 2024). This could enhance the efficiency of key fungal groups in executing specific processes, such as lignin degradation or SON transformation (Yang et al. 2025). On the other hand, the decline in connectivity may also reflect impaired fungal resilience to environmental disturbances (Hannula et al., 2025). We propose that although BC amendment partially counteracted AR-induced soil acidification, it also intensified niche competition and functional differentiation among fungi, ultimately driving the assembly of a sparser and more specialized network (Zhou et al. 2022).

Notably, essential shifts included increased abundance of Proteobacteria (i.e., N fixers) (Zhang et al. 2020) and decreased abundance of Acidobacteriota (Fig. S4). Stimulation of those two phyla by exogenous OM has been reported previously (Yang et al. 2022; Feng et al. 2022). Acidobacteria are considered to be acidophilic oligotrophic bacteria that grow and decompose relatively recalcitrant materials (e.g., lignin, aromatic C, and olefin C) contained in the soil (Watzinger et al. 2014). The reduction in its relative abundance under AR conditions after the BC amendment explains the sequestration of soil C. Basidiomycota remained the dominant fungal phylum (Fig. S5), consistent with acidic soil ecotypes (Muneer et al. 2021). Fungal network reduction may reflect AR-induced soil dysbiosis (Yuan et al. 2020), while suppressed Ascomycota (i.e., humic acid biomarkers often associated with pathogens) suggests altered C and N cycling (Jin et al. 2022). Notably, BC altered microbial metabolic pathways, warranting metagenomic validation to quantify functional gene responses.

4.3 Mechanism of BC-mediated AHN regulation under AR stress

Contrary to the generally observed inverse relationship between soil AHN content and pH (Jia et al. 2024), we observed that the application of alkaline BC increased AHN while simultaneously raising soil pH (Figs. 1 and 2). This apparent paradox can be explained by distinguishing between the direct and indirect effects of BC on soil properties (Tang et al. 2025). The increase in soil pH may be primarily a direct effect attributable to the inherent alkalinity of the BC itself, which originates from its carbonates, ash, and the substantial content of base cations such as Ca (Fig. S6). The dissolution and hydrolysis of these alkaline components, including $CaO/Ca(OH)_2$ derived from the biogenic Ca in the *Q. acutissima* leaf feedstock, may directly neutralize soil acidity (Xu et al. 2013).

In contrast, the enhancement of AHN content may be mainly driven by a series of indirect effects mediated by BC. Firstly, the pH increase promotes deprotonation of oxygen-containing functional groups (–OH, $–COO^-$) on BC surfaces, enhancing anion exchange capacity and facilitating complexation with organic N molecules, thereby stabilizing AHN fractions (Wang et al. 2024). Secondly, BC-mediated acid stress alleviation may improve microbial growth and N use efficiency, increasing the production and preservation of acid-hydrolyzable microbial residues (e.g., amino sugars) that directly contribute to the AHN pool (Parasar et al., 2025).

Notably, the response pattern of soil EC provides further support for the predominance of these indirect effects. Under AR conditions, BC amendment resulted in a decrease in EC (Fig. 2), indicating that its indirect effects (e.g., promoting microbial immobilization of ions and retaining soluble nutrients through its porous structure) outweighed the direct contribution of soluble salts from the BC itself (Sadegh-Zadeh et al. 2018).

BC application significantly enhanced soil AN content under AR stress by optimizing soil conditions and microbial N utilization. RF analysis identified soil chemical properties (e.g., DTN and pH) as primary regulators of AN dynamics (Fig. 6). Although AR typically exacerbates N leaching (Wen et al. 2024), BC counteracted this by increasing microbial NUE, thereby maintaining soil available N. This inference was further supported by PLS-PM analysis (Fig. 7).

Soil ASN and AAN accumulation were co-regulated by MBN and LAP activity (Fig. 6). Enhanced MBN reflects greater microbial N assimilation, where active organic N is converted to microbial biomass and subsequently stabilized as ASN and AAN through necromass pathways (e.g., intracellular N compounds) (Liu et al. 2025). Concurrently, BC-stimulated LAP activity catalyzes protein/peptide hydrolysis into amino acids, directly supplying AAN precursors (Yu et al. 2021). Thus, MBN (necromass pathway) and LAP (substrate conversion) synergistically drive AHN enrichment.

The positive correlation between soil AUN and NAG activity (Fig. 5) indicates a synergistic relationship in BC-amended soil. NAG primarily participates in the

degradation of chitin and other amino polysaccharides (Xia et al. 2025). Enhanced NAG activity likely accelerates the depolymerization of labile SON, generating precursors that promote the formation of more stable N (i.e., AUN) (Zhou et al. 2023). Thus, BC may trigger a priming effect whereby NAG-mediated decomposition ultimately channels more N into stable AUN pools, highlighting its role in redirecting microbial enzymatic pathways toward long-term N sequestration.

4.4 Research limitations and implications for BC amendment under AR stress

Notably, the observed increases in soil TN and AHN components under BC amendment likely result from a combination of direct N input from the BC itself and its indirect mediation of soil N processes. N-containing BC may directly supplement the soil N pool. Nevertheless, it is challenging to distinguish BC-derived N from native soil N under field conditions. Therefore, the overall effect of BC represents an integration of external N input and enhanced retention of indigenous N. Future studies using ^{15}N isotopic tracing are needed to quantitatively partition the BC-derived N and track its allocation across mineral N, SON, and AHN fractions.

Moreover, the environmental risks posed by AR to plantation forest soil ecosystems warrant serious attention. In light of increasing AR pollution, the application of engineered BC (e.g., pyrochar) may exert positive ecosystem-level influences on soil C and N cycling. Our findings thus provide a scientific basis for predicting biogeochemical cycles under global change and for developing targeted AR mitigation strategies. To advance practical implementation, the following limitations and research priorities warrant further investigation: (1) The low background pH of the selected *Q. acutissima* plantations may modulate BC efficacy. Controlled experiments across soil pH gradients are needed to dissect BC-mediated N dynamics under AR stress. (2) High-resolution depth-resolved sampling must quantify BC-induced N sequestration profiles, assessing long-term efficacy against AR constituent leaching. (3) Integrating ^{15}N tracing and climate projections will elucidate the role of BC in mitigating gaseous N losses (e.g., N_2O) while stabilizing labile N pools under dynamic AR scenarios.

5 Conclusion

This study demonstrates that biochar (BC) application effectively mitigated acid rain (AR) stress on acid-hydrolyzable nitrogen (N) fractions. Specifically, BC significantly enhanced acid-ammonium N, acid-amino acid N, acid-amino sugar N, and acid-hydrolyzable unidentified N accumulation. The regulatory effect was driven by chemo-biological synergy with multi-model validation confirming biological dominance. Under AR stress, the BC amendment increased the complexity of the bacterial network, contrasting with the simultaneous simplification of the fungal network. Crucially, positive regulatory effects of BC on soil acid-hydrolyzable N fractions surpassed AR-induced negative impacts. These findings advance the biogeochemical understanding of N cycling in AR-affected soils and establish a mechanistic framework for sustainable N management in plantation ecosystems.

Abbreviations

AHN	Acid-hydrolysable nitrogen
SON	Soil organic nitrogen
AN	Acid-ammonia nitrogen
AAN	Acid-amino acid nitrogen
ASN	Acid-amino sugar nitrogen
AUN	Acid-hydrolyzable unidentified nitrogen
AR	Acid rain
BC	Biochar
C	Carbon
N	Nitrogen
CK	Control without BC application and AR spraying
AR-BC	Treatments with BC application and AR spraying
OC	Organic carbon
TN	Total nitrogen
SSA	Specific surface area
OM	Organic matter
SOC	Soil organic carbon
EC	Electrical conductivity
DOC	Dissolved organic carbon
DTN	Dissolved total nitrogen
BG	β-Glucosidase
NAG	β-N-acetylglucosaminidase
AP	Acid phosphatase
LAP	Leucine aminopeptidase
CUE	Microbial carbon use efficiency
NUE	Microbial nitrogen use efficiency
TER	Threshold element ratio
VPA	Variance decomposition analysis
RF	Random forest
PLS-PM	Partial least squares path model

Supplementary Information

The online version contains supplementary material available at https://doi.org/10.1007/s42773-026-00572-5.

Additional file 1.

Acknowledgements
The authors thank the valuable comments of anonymous reviewers and Editor.

Author contributions
Yuanyuan Feng: Conceptualization, Writing-original draft, Data curation. Yuanhao Liu: Writing-original draft, Data curation. Jiaxuan Liu: Writing—review and editing. Haibo Hu: Supervision, Funding acquisition, Writing—review and editing. Meijia Zhou: Writing—review and editing. Yanfang Feng: Writing—review and editing. Lihong Xue: writing—review and editing. The authors read and approved the final manuscript.

Funding
This work was supported by the Jiangsu Province Carbon Peak and Carbon Neutrality and Technology Innovation Special Fund Project (BE2022305), National Positioning Observation and Research Project

of Farmland Protection Forest Ecosystem in Changjiang River Delta (2024132088), Basic Research Program of Jiangsu (BK20250692) and Natural Science Foundation of the Jiangsu Higher Education Institutions of China (25KJB210009).

Data availability
Data will be made availability on request.

Declarations

Ethics approval and consent to participate
Not applicable.

Consent for publication
All listed authors have approved the manuscript before submission.

Competing interests
The authors declare that they have no known competing financial interests or personal relationships that could have appeared to influence the work reported in this paper.

Author details
[1]Co-Innovation Center for Sustainable Forestry in Southern China, College of Forestry and Grassland, Nanjing Forestry University, Nanjing 210037, China. [2]Key Laboratory of Agro-Environment in Downstream of Yangtze Plain, National Agricultural Experiment Station for Agricultural Environment (Luhe), Ministry of Agriculture and Rural Affairs, Institute of Agricultural Resources and Environment, Jiangsu Academy of Agricultural Sciences, Nanjing 210014, China.

Received: 17 June 2025 Revised: 19 December 2025 Accepted: 5 January 2026
Published online: 15 February 2026

References

Arwenyo B, Varco JJ, Dygert A, Brown S, Pittman CU, Mlsna T (2023) Contribution of modified p-enriched biochar on ph buffering capacity of acidic soil. J Environ Manage 339:117863. https://doi.org/10.1016/j.jenvman.2023.117863

Chen S, Elrys AS, Yang W, Du S, He M, Cai Z, Zhang J, Müller C (2024a) Soil recalcitrant but not labile organic nitrogen mineralization contributes to microbial nitrogen immobilization and plant nitrogen uptake. Glob Change Biol. https://doi.org/10.1111/gcb.17290

Chen Y, Sun K, Yang Y, Gao B, Zheng H (2024b) Effects of biochar on the accumulation of necromass-derived carbon, the physical protection and microbial mineralization of soil organic carbon. Crit Rev Environ Sci Technol 54:39–67. https://doi.org/10.1080/10643389.2023.2221155

Cheng Y, Zhang S, Song D, Wu H, Wang L, Wang X (2023) Distribution characteristics of microbial residues within aggregates of fluvo-aquic soil under biochar application. Agron J 13:392. https://doi.org/10.3390/agronomy13020392

Du B, Kiese R, Butterbach-Bahl K, Dirnböck T, Rennnenberg H (2025) Consequences of nitrogen deposition and soil acidification in European forest ecosystems and mitigation approaches. For Ecol Manage 580:122523. https://doi.org/10.1016/j.foreco.2025.122523

Feng Y, Han L, Li D, Sun M, Wang X, Xue L, Poinern G, Feng Y, Xing B (2022) Presence of microplastics alone and co-existence with hydrochar unexpectedly mitigate ammonia volatilization from rice paddy soil and affect structure of soil microbiome. J Hazard Mater 422:126831. https://doi.org/10.1016/j.jhazmat.2021.126831

Feng Y, Tang Q, Xie W, Yu J, Wang L, Wang B, Xie H, Zhang M, Bo L, Jin H, Feng Y, Xue L (2025) Application of products derived from pyrolysis and hydrothermal carbonization as conditioners for aerobic composting produced multiple beneficial effects: evaluation based on 10-ton pilot scale trials. Chem Eng J. https://doi.org/10.1016/j.cej.2025.159793

Hannula SE, Veen GF (2025) Drought has short-term effects on soil fungal communities leading to long-term effects on soil functions. Soil Biol Biochem 209:109893. https://doi.org/10.1016/j.soilbio.2025.109893

He Z, Cao H, Liang J, Hu Q, Zhang Y, Nan X, Li Z (2022) Effects of biochar particle size on sorption and desorption behavior of NH_4^+-N. Ind Crops Prod 189:115837. https://doi.org/10.1016/j.indcrop.2022.115837

Jia X, Ma H, Yan W, Shangguan Z, Zhong Y (2024) Effects of co-application of biochar and nitrogen fertilizer on soil profile carbon and nitrogen stocks and their fractions in wheat field. J Environ Manage 368:122140. https://doi.org/10.1016/j.jenvman.2024.122140

Jin Q, Zhang Y, Wang Q, Li M, Sun H, Liu N, Zhang L, Zhang Y, Liu Z (2022) Effects of potassium fulvic acid and potassium humate on microbial biodiversity in bulk soil and rhizosphere soil of *Panax ginseng*. Microbiol Res 254:126914. https://doi.org/10.1016/j.micres.2021.126914

Knorr MA, Contosta AR, Morrison EW, Muratore TJ, Anthony MA, Stoica I, Geyer KM, Simpson MJ, Frey SD (2024) Unexpected sustained soil carbon flux in response to simultaneous warming and nitrogen enrichment compared with single factors alone. Nat Ecol Evol 8:2277–2285. https://doi.org/10.1038/s41559-024-02546-xLee

Lee BR, Park SH, Muchlas M, Kim TH (2025) Comparative effectiveness of zeolite and rice husk biochar in mitigating NH_3 and N_2O emissions as linked to the nitrogen use efficiency of pig slurry during the vegetative growth of Brassica napus. Chem Biol Technol Agric 12(1):131. https://doi.org/10.1186/s40538-025-00859-y

Li JT, Zhang Y, Chen H, Sun H, Tian W, Li J, Liu X, Zhou S, Fang C, Li B, Nie M (2023) Low soil moisture suppresses the thermal compensatory response of microbial respiration. Glob Change Biol 29:874–889. https://doi.org/10.1111/gcb.16448

Li J, Wu J, Yu J, Wang K, Li J, Cui Y, Shangguan Z, Deng L (2024) Soil enzyme activity and stoichiometry in response to precipitation changes in terrestrial ecosystems. Soil Biol Biochem 191:109321. https://doi.org/10.1016/j.soilbio.2024.109321

Lin X, Yang Y, Yang P, Hong Y, Zhang L, Tong C, Lai DYF, Lin Y, Tan L, Tian Y, Tang KW (2023) Soil organic nitrogen content and composition in different wetland habitat types along the south-east coast of China. Catena 232:107457. https://doi.org/10.1016/j.catena.2023.107457

Liu J, Jiang B, Shen J, Zhu X, Yi W, Li Y, Wu J (2021) Contrasting effects of straw and straw-derived biochar applications on soil carbon accumulation and nitrogen use efficiency in double-rice cropping systems. Agr Ecosyst Environ 311:107286. https://doi.org/10.1016/j.agee.2020.107286

Liu S, Cen B, Yu Z, Qiu R, Gao T, Long X (2025) The key role of biochar in amending acidic soil: reducing soil acidity and improving soil acid buffering capacity. Biochar. https://doi.org/10.1007/s42773-025-00432-8

Marinos RE, Groffman PM, Driscoll CT, Bernhardt ES (2024) Accelerated soil nitrogen cycling in response to a whole ecosystem acid rain mitigation experiment. Soil Biol Biochem 189:109286. https://doi.org/10.1016/j.soilbio.2023.109286

Mooshammer M, Wanek W, Hämmerle I, Fuchslueger L, Hofhansl F, Knoltsch A, Schnecker J, Takriti M, Watzka M, Wild B, Keiblinger KM, Zechmeister-Boltenstern S, Richter A (2014) Adjustment of microbial nitrogen use efficiency to carbon:nitrogen imbalances regulates soil nitrogen cycling. Nat Commun. https://doi.org/10.1038/ncomms4694

Muneer MA, Huang X, Hou W, Zhang Y, Cai Y, Munir MZ, Wu L, Zheng C (2021) Response of fungal diversity, community composition, and functions to nutrients management in red soil. J Fungi. https://doi.org/10.3390/jof7070554

Ning Y, Li S, Ning C, Ren J, Xia Z, Zhu M, Gao Y, Zhang X, Ma Q, Yu W (2025) Effects of exogenous nitrogen addition on soil organic nitrogen fractions in different fertility soils: result from a ^{15}N cross-labeling experiment. Agr Ecosyst Environ 379:109366. https://doi.org/10.1016/j.agee.2024.109366

Parasar BJ, Agarwala N (2025) Unravelling the role of biochar-microbe-soil tripartite interaction in regulating soil carbon and nitrogen budget: a panacea to soil sustainability. Biochar 7(1):37. https://doi.org/10.1007/s42773-024-00411-5

Qi S, Degen A, Wang W, Huang M, Li D, Luo B, Xu J, Dang Z, Guo R, Shang Z (2024) Systemic review for the use of biochar to mitigate soil degradation. GCB Bioenergy. https://doi.org/10.1111/gcbb.13147

Ren G, Zhang X, Xin X, Yang W, Zhu A, Yang J, Li M (2023) Soil organic carbon and nitrogen fractions as affected by straw and nitrogen management on the north China plain. Agric Ecosyst Environ 342:108248. https://doi.org/10.1016/j.agee.2022.108248

Sadegh-Zadeh F, Parichehreh M, Jalili B, Bahmanyar MA (2018) Rehabilitation of calcareous saline-sodic soil by means of biochars and acidified biochars. Land Degrad Dev 29(10):3262–3271. https://doi.org/10.1002/ldr.3079

Shi R, Liu Z, Li Y, Jiang T, Xu M, Li J, Xu R (2019) Mechanisms for increasing soil resistance to acidification by long-term manure application. Soil Tillage Res 185:77–84. https://doi.org/10.1016/j.still.2018.09.004

Silverstein MR, Bhatnagar JM, Segrè D (2024) Metabolic complexity drives divergence in microbial communities. Nat Ecol Evol 8(8):1493–1504. https://doi.org/10.1038/s41559-024-02440-6

Sinsabaugh RL, Turner BL, Talbot JM, Waring BG, Powers JS, Kuske CR, Moorhead DL, Shah JJF (2016) Stoichiometry of microbial carbon use efficiency in soils. Ecol Monogr 86(2):172–189. https://doi.org/10.1890/15-2110.1

Sun Y, Wang C, Ruan H (2022) Increased microbial carbon and nitrogen use efficiencies under drought stress in a poplar plantation. For Ecol Manage 519:120341. https://doi.org/10.1016/j.foreco.2022.120341

Tang R, Yao S, Liu Y, Ren T, Ma J, Gong X, Li G, Ma R, Yuan J (2025) Iron-modified biochar enhanced nitrogen retention during composting:bridging chemisorption and microbiome modulation. Chem Eng J 513:162761. https://doi.org/10.1016/j.cej.2025.162761

Toczydlowski AJZ, Slesak RA, Venterea RT, Spokas KA (2023) Pyrolysis temperature has greater effects on carbon and nitrogen biogeochemistry than biochar feedstock when applied to a sandy forest soil. Forest Ecol Manag 534:120881. https://doi.org/10.1016/j.foreco.2023.120881

Wang D, Lan Y, Chen W, Han X, Liu S, Cao D, Cheng X, Wang Q, Zhan Z, He W (2023) The six-year biochar retention interacted with fertilizer addition alters the soil organic nitrogen supply capacity in bulk and rhizosphere soil. J Environ Manage 338:117757. https://doi.org/10.1016/j.jenvman.2023.117757

Wang D, Lan Y, Chen W, Liu Z, Gao J, Cao D, Wang Q, Mazhang C, An X (2024) Response of bacterial communities, enzyme activities and dynamic changes of soil organic nitrogen fractions to six-year different application levels of biochar retention in Northeast China. Soil Tillage Res 240:106097. https://doi.org/10.1016/j.still.2024.106097

Wang X, Zou T, Lian J, Chen Y, Cheng L, Hamid Y, He Z, Jeyakumar P, Yang X, Wang H (2025) Simultaneous mitigation of cadmium contamination and greenhouse gas emissions in paddy soil by iron-modified biochar. J Hazard Mater 488:137430. https://doi.org/10.1016/j.jhazmat.2025.137430

Watzinger A, Feichtmair S, Kitzler B, Zehetner F, Kloss S, Wimmer B, Zechmeister-Boltenstern S, Soja G (2014) Soil microbial communities responded to biochar application in temperate soils and slowly metabolized ^{13}C-labelled biochar as revealed by ^{13}C PLFA analyses: results from a short-term incubation and pot experiment. Eur J Soil Sci 65(1):40–51. https://doi.org/10.1111/ejss.12100

Wen Z, Ma X, Xu W, Si R, Liu L, Ma M, Zhao Y, Tang A, Zhang Y, Wang K, Zhang Y, Shen J, Zhang L, Zhao Y, Zhang F, Goulding K, Liu X (2024) Combined short-term and long-term emission controls improve air quality sustainably in China. Nat Commun 15:5169

Wu J, Xiong X, Hui D, Zhang H, Li J, Chang Z, Zhang S, Su Y, Li X, Zhang D, Deng Q (2024) Soil aggregate size distribution mediates microbial responses to prolonged acid deposition in a subtropical forest in south China. Soil Biol Biochem 198:109544. https://doi.org/10.1016/j.soilbio.2024.109544

Xia Y, Chen X, Zheng S, Gunina A, Ning Z, Hu Y, Tang H, Rui Y, Zhang Z, He H, Huang D, Su Y (2021) Manure application accumulates more nitrogen in paddy soils than rice straw but less from fungal necromass. Agr Ecosyst Environ 319:107575. https://doi.org/10.1016/j.agee.2021.107575

Xia Y, Gao P, Lei W, Gao J, Luo Y, Peng F, Mou T, Zhao Z, Zhang K, Guggenberger G, Zhang H, Zhang Z (2025) Covering green manure increases rice yields via improving nitrogen cycling between soil and crops in paddy fields. Agr Ecosyst Environ 383:109517. https://doi.org/10.1016/j.agee.2025.109517

Xu G, Wei LL, Sun JN, Shao HB, Chang SX (2013) What is more important for enhancing nutrient bioavailability with biochar application into a sandy soil: direct or indirect mechanism? Ecol Eng 52:119–124. https://doi.org/10.1016/j.ecoleng.2012.12.091

Xu J, Ren C, Zhang X, Wang C, Wang S, Ma B, He Y, Hu L, Liu X, Zhang F, Lu L, Li S, Zhang J, Zhu Y, Vitousek P, Gu B (2025) Soil health contributes to variations in crop production and nitrogen use efficiency. Nat Food. https://doi.org/10.1038/s43016-025-01155-6

Yang Y, Sun K, Liu J, Chen Y, Han L (2022) Changes in soil properties and CO_2 emissions after biochar addition: role of pyrolysis temperature and aging. Sci Total Environ 839:156333. https://doi.org/10.1016/j.scitotenv.2022.156333

Yang J, Wang Z, Liu Z, Chang Q, Wang B, Zhang Y, Bai E (2025) Intensified aridity hinders soil microbes from improving their nitrogen use efficiency. Glob Chang Biol 31(8):e70453. https://doi.org/10.1111/gcb.70453

Yu H, Liu X, Yang C, Peng Y, Yu X, Gu H, Zheng X, Wang C, Xiao F, Shu L, He Z, Wu B, Yan Q (2021) Co-symbiosis of arbuscular mycorrhizal fungi (AMF) and diazotrophs promote biological nitrogen fixation in mangrove ecosystems. Soil Biol Biochem 161:108382. https://doi.org/10.1016/j.soilbio.2021.108382

Yu G, Zheng M, Wang YP, Yu M, Jiang J, Hou E, Cao N, Ye S, Chen S, Wu J, Liu F, Wang L, Zhang S, Xu P, Zhang D, Yan J (2025) Trees show higher resilience than herbs under phosphorus deficit induced by 12-year simulated acid rain. Ecology. https://doi.org/10.1002/ecy.70071

Yuan J, Wen T, Zhang H, Zhao M, Penton CR, Thomashow LS, Shen Q (2020) Predicting disease occurrence with high accuracy based on soil macroecological patterns of Fusarium wilt. ISME J 14(12):2936–2950. https://doi.org/10.1038/s41396-020-0720-5

Zhang X, Jia X, Wu H, Li J, Yan L, Wang J, Li Y, Kang X (2020) Depression of soil nitrogen fixation by drying soil in a degraded alpine peatland. Sci Total Environ 747:141084. https://doi.org/10.1016/j.scitotenv.2020.141084

Zhang Y, Xie H, Wang F, Sun C, Zhang X (2022) Effects of biochar incorporation on soil viable and necromass carbon in the luvisol soil. Soil Use Manage 38:318–330. https://doi.org/10.1111/sum.12720

Zhou M, Hu H, Wang J, Zhu Z, Feng Y (2022) Nitric acid rain increased bacterial community diversity in north subtropical forest soil. Forests 13(9):1349. https://doi.org/10.3390/f13091349

Zhou M, Hu H, Wang J, Wang X, Tian Z, Deng W, Wu C, Zhu L, Lu Q, Feng Y (2023) Effects of nitric acid rain stress on soil nitrogen fractions and fungal communities in a northern subtropical forest, China. Sci Total Environ 856:158904. https://doi.org/10.1016/j.scitotenv.2022.158904